

# Pharmacological modulation of ventral tegmental area neurons elicits changes in trigeminovascular sensory processing and is accompanied by glycemic changes: Implications for migraine

Cephalalgia

42(13) 1–16

© International Headache Society 2022





Article reuse guidelines:

sagepub.com/journals-permissions

DOI: 10.1177/03331024221110111

journals.sagepub.com/home/cep



Margarida Martins-Oliveira<sup>1,2,3,4</sup>, Simon Akerman<sup>5</sup> ,  
Philip R Holland<sup>1</sup>, Isaura Tavares<sup>3,4</sup> and Peter J Goadsby<sup>1,6</sup> 

## Abstract

**Background:** Imaging migraine premonitory studies show increased midbrain activation consistent with the ventral tegmental area, an area involved in pain modulation and hedonic feeding. We investigated ventral tegmental area pharmacological modulation effects on trigeminovascular processing and consequent glycemic levels, which could be involved in appetite changes in susceptible migraine patients.

**Methods:** Serotonin and pituitary adenylate cyclase-activating polypeptide receptors immunohistochemistry was performed in ventral tegmental area parabrachial pigmented nucleus of male Sprague Dawley rats. *In vivo* trigeminocervical complex neuronal responses to dura mater nociceptive electrical stimulation, and facial mechanical stimulation of the ophthalmic dermatome were recorded. Changes in trigeminocervical complex responses following ventral tegmental area parabrachial pigmented nucleus microinjection of glutamate, bicuculline, naratriptan, pituitary adenylate cyclase-activating polypeptide-38 and quinpirole were measured, and blood glucose levels assessed pre- and post-microinjection.

**Results:** Glutamatergic stimulation of ventral tegmental area parabrachial pigmented nucleus neurons reduced nociceptive and spontaneous trigeminocervical complex neuronal firing. Naratriptan, pituitary adenylate cyclase-activating polypeptide-38 and quinpirole inhibited trigeminovascular spontaneous activity, and trigeminocervical complex neuronal responses to dural-evoked electrical and mechanical noxious stimulation. Trigeminovascular sensory processing through modulation of the ventral tegmental area parabrachial pigmented nucleus resulted in reduced circulating glucose levels.

**Conclusion:** Pharmacological modulation of ventral tegmental area parabrachial pigmented nucleus neurons elicits changes in trigeminovascular sensory processing. The interplay between ventral tegmental area parabrachial pigmented nucleus activity and the sensory processing by the trigeminovascular system may be relevant to understand associated sensory and homeostatic symptoms in susceptible migraine patients.

## Keywords

Ventral tegmental area, migraine, nociception, blood glucose, naratriptan, PACAP

Date received: 6 January 2022; revised: 24 April 2022; accepted: 24 May 2022

<sup>1</sup>Headache Group, Wolfson Centre for Age-Related Disease, Institute of Psychiatry, Psychology and Neuroscience, King's College London, UK

<sup>2</sup>Department of Nutrition and Metabolism, NOVA Medical School| Faculdade de Ciências Médicas, NMS|FCM, Universidade Nova de Lisboa; Lisboa, Portugal

<sup>3</sup>Department of Biomedicine, Faculty of Medicine of University of Porto, Porto, Portugal

<sup>4</sup>Institute of Investigation and Innovation in Health (i3S), University of Porto, Porto, Portugal

<sup>5</sup>Department of Neural and Pain Sciences, University of Maryland Baltimore, Baltimore, Maryland, USA

<sup>6</sup>Department of Neurology, University of California, Los Angeles, Los Angeles CA USA

## Corresponding author:

Peter J Goadsby, Headache Group, Wolfson Centre for Age-Related Disease, Institute of Psychiatry, Psychology and Neuroscience, Wellcome Foundation Building, King's College Hospital, London, SE5 9PJ, UK.  
Email: peter.goadsby@kcl.ac.uk

## Introduction

Human imaging studies have shown that several areas of the brain (e.g. hypothalamus, ventral tegmental area (VTA), nucleus accumbens (NAc)) are active during the premonitory phase of spontaneous migraine (1,2), and in nitroglycerin-induced migraine attacks (3). The midbrain VTA is involved in goal-directed behavior and in processing for natural rewards (e.g. food reward), alcohol and drugs of abuse, and is further linked to pain modulation (4–7). Recently, a connection between the periaqueductal grey (PAG) matter and the VTA has shown to mediate aversive behavior in an inflammatory model of headache (8).

The VTA is a heterogeneous nucleus containing dopaminergic (DA) neurons ( $\approx 65\%$ ) with reciprocal projections to several nuclei including the NAc, prefrontal cortex, amygdala, hypothalamus and periaqueductal gray (PAG) (9). It also contains GABAergic ( $\approx 30\%$ ) and glutamatergic (GLU) neurons ( $\approx 5\%$ ) (10–13), that regulate local VTA DA neuronal activity, but also have projection targets similar to those of DA neurons (14–19). It exhibits antero-posterior anatomical and functional heterogeneity with topographic neuronal projections (6,20). Specifically, the parabrachial pigmented nucleus of the VTA (VTA<sup>PBP</sup>) (21,22), sends neuronal projections to the medial prefrontal cortex (mPFC), and medial and lateral shell of the NAc (23–26). We hypothesized that modulation of the VTA may influence trigeminovascular processing, which could be involved in appetite changes in susceptible migraine patients (27,28). We used an animal model of acute dural nociceptive activation of the trigeminovascular system, which has reliably predicted clinical efficacy of migraine therapeutics (29). The literature reports the location of migraine-relevant 5-HT<sub>1</sub> and pituitary adenylate cyclase activating polypeptide (PACAP) receptors within the VTA (by using *in situ* hybridization (30), quantitative autoradiographic mapping (31) or by immunohistochemistry and by double immunofluorescence (32)) but was inconsistent about the location specifically within the VTA subnuclei, namely the VTA<sup>PBP</sup>. Hence, we first used immunofluorescence to perform a topographic evaluation of the expression of 5-HT<sub>1B</sub>, 5-HT<sub>1D</sub>, PAC<sub>1</sub>, VPAC<sub>1</sub> and VPAC<sub>2</sub> receptors in the VTA<sup>PBP</sup> and to guide pharmacological administration. We then studied the effects of the modulation of excitatory and inhibitory inputs within the VTA<sup>PBP</sup> on trigeminovascular neuronal responses by manipulating VTA<sup>PBP</sup> neurons with glutamate and a competitive antagonist of GABA<sub>A</sub> receptors. We further investigated potential therapeutic modulation by microinjecting naratriptan, a 5-HT<sub>1B/D/F</sub> receptor agonist widely used in migraine treatment; PACAP38, a peptide that, when administered

intravenously, induces delayed migraine-like headaches in susceptible migraine patients (33); and a DA D<sub>2</sub>/D<sub>3</sub> receptor agonist, known to inhibit trigeminovascular responses in animals (34). Since trigeminal cell activation has been associated with blood glucose changes *in vivo* (28,35), we further explored whether peripheral glucose levels were influenced by trigeminovascular sensory processing through modulation of VTA<sup>PBP</sup> neurons. Preliminary results have been previously presented (36,37).

## Materials and methods

All experiments were conducted in agreement with the guidelines of the Institutional Animal Care and Use Committee (University of California, San Francisco), the UK Home Office Animals (Scientific Procedures) Act 1986, the ARRIVE guidelines (38) and the Committee for Research and Ethical Issues of International Association for the Study of Pain (39). Male Sprague Dawley rats were group-housed and maintained under standard conditions (12 h light–dark cycles; lights ON at 07:00) with food and water available *ad libitum*. The subjective bias when allocating the animals to the experimental groups was minimized by arbitrarily housing the animals in pairs upon their arrival, then the animals were randomly picked from the cage for each procedure. To avoid confounding effects regarding the diurnal cycle, all experiments initiated between 8.00–9.00 am.

### *Immunohistofluorescence characterization of the VTA<sup>PBP</sup>*

Animals (315–330 g,  $n = 4$ ; Charles River, France) were euthanized with pentobarbital sodium and perfused with 250 ml of heparinized phosphate-buffered saline through the ascending aorta, followed by 300 ml of a fixative solution containing 4% paraformaldehyde. The brain was removed and fixated (35). Serial coronal sections (30  $\mu\text{m}$ -thick) containing the VTA<sup>PBP</sup>, hypothalamus or PAG were cut on a cryostat and processed. Staining was visualized using a fluorescence microscope coupled to digital camera and image software (AxioVision 4.8.2, Carl Zeiss). Briefly, sections were washed in phosphate buffered saline (PBS) and after 60 min incubation in a blocking solution of PBS, 5% normal goat serum (Sigma-Aldrich), and 0.25% Triton x-100 (Alfa Aesar), sections were incubated overnight at 4°C with primary antibody specific to 5-HT<sub>1B</sub> or 5-HT<sub>1D</sub> receptors (1:75; ASR-022; ASR-023; Alomone Labs). Sections were washed and incubated in goat anti-rabbit Fluorescein for 90 min (1:250; FI-1000, Vector Laboratories). Another set of sections were washed in PBS, incubated for 30 minutes in PBS with

1% sodium borohydride (Sigma-Aldrich) and washed in PBS. After 60 min incubation in a blocking solution of PBS, 5% normal goat or horse serum (Sigma-Aldrich), and 0.25% Triton x-100, sections were incubated overnight at 4°C with primary antibody specific to PAC<sub>1</sub>, VPAC<sub>1</sub> and VPAC<sub>2</sub> receptors (1:100; AVR-003; AVR-001; AVR-002; Alomone Labs), made up in PBS, 2% normal goat or horse serum (Vector Laboratories), and 0.25% Triton x-100. Sections were washed and incubated for 90 min in donkey anti-rabbit Alexa Fluor 594 (for PAC<sub>1</sub> and VPAC<sub>2</sub>, 1:1000, Life Technologies Corporation) or goat anti-rabbit Texas Red (for VPAC<sub>1</sub>, 1:1000, TI-1000, Vector Laboratories). Sections were then mounted with DAPI. Primary antibodies were chosen based on recent published studies (40–43) and the specificity was demonstrated by the suppliers. Additionally, samples were processed with the omission of primary antibodies, and the staining of brain areas known to contain each receptor was performed.

### *In vivo electrophysiology*

The surgical preparation and recording setup has been detailed previously (44). Briefly, animals (270–340 g,  $n = 70$ , Charles River, USA or UK) were anesthetized with 5% (v/v) isoflurane (induction) and propofol solution (maintenance). Body temperature, respiratory rate, end-tidal CO<sub>2</sub> and blood pressure were continuously monitored. After fixation of the skull in a stereotaxic frame rats were ventilated with oxygen-enriched air.

To access the dura mater and middle meningeal artery (MMA), a craniotomy was performed with a saline-cooled drill and the underlying dura mater covered in mineral oil. To access the TCC, muscles of the dorsal neck were separated, a cervical (C1) laminectomy performed, and the dura mater incised to expose the caudal medulla oblongata. A piezo-electric microelectrode positioner was used to locate the optimal recording site within the TCC. Animals were left to stabilize for at least 60 min before recordings.

A bipolar stimulating electrode connected to a stimulus isolation unit was placed on the intact dura mater adjacent to the MMA for electrical stimulation of the perivascular afferents of the trigeminal nerve (Figure 1A). Stimulation of primary trigeminal afferents was performed with supramaximally square wave pulses generated by a Grass S88 stimulator. Dural nociceptive neurons in the TCC were identified via electrical stimuli (9–15 V, 0.15–0.3 ms, 0.4–0.5 Hz, 20 sweeps), activating trigeminal A $\delta$ -fibers with approximate latencies between 4–20 ms. By using low stimulation parameters, we activated only A $\delta$ -fibers.

Extracellular recordings were made from wide dynamic range (WDR) neurons in the TCC, activated

by dural stimulation using tungsten microelectrodes. Neurons were characterized for their cutaneous and deep receptive fields. The cutaneous receptive field was assessed in all three territories of the trigeminal innervation (Figure 1B) and was identified as the recording electrode was advanced in the spinal cord. The receptive field was assessed for both innocuous (gentle brush), and noxious inputs (pinch) (Figure 1D). When a neuron sensitive to stimulation of the ophthalmic (V1) dermatome of the trigeminal nerve was identified it was tested for convergent input from the dura mater.

### *Drugs and microinjections*

Animals were microinjected unilaterally into the VTA<sup>PBP</sup>, ipsilateral to the recording site in the TCC, with glutamate (50 mM; Sigma-Aldrich); bicuculline (2 mM; Tocris Bioscience); naratriptan (25 mM; Sigma-Aldrich); pituitary adenylate cyclase activating polypeptide (PACAP38; 100  $\mu$ M; Tocris Bioscience); quinpirole (4  $\mu$ g in 400 nL; Sigma-Aldrich); or saline as vehicle control. All drugs were dissolved in sterile saline solution (0.9% sodium chloride, Baxter International Inc.). On the day of the experiment, drugs were dissolved in 2% of dye (Chicago Sky Blue 6B, Alfa Aesar), except for naratriptan and quinpirole due to dissolving difficulties. Volumes were given in a range of 300–400 nL. Doses were chosen based on previous studies (45–47). An area of bone directly above the coordinates of the VTA<sup>PBP</sup> was thinned and removed and the dura mater pierced to allow entry of a microliter syringe (Figure 1A). The VTA<sup>PBP</sup> stereotaxic coordinates were: from bregma, AP 5.3 mm; ML  $\pm$ 0.7 mm; DV-7.5 mm from dura mater (22). The microinjection sites were either marked by deposition of dye or by the syringe track with blood (naratriptan and quinpirole administration). We also performed preliminary studies to confirm there was no spread of the dye solution outside the target area (data not shown). The location of the injection and dye was restricted to the target area of VTA<sup>PBP</sup> in a longitudinal manner and did not reach the posterior hypothalamus (anterior to the VTA<sup>PBP</sup>) or the substantia nigra compacta (lateral to the VTA<sup>PBP</sup>).

### *Blood glucose levels*

Tail vein blood glucose was quantified using a glucometer (FreeStyle Lite, Abbott Diabetes Care Inc). Given that a non-diabetic animal was used and there was no indication of VTA direct effects on glycemia, single time-point blood glucose measurements were performed, as reported in clinical (48,49) and rodent (35) migraine studies. To confirm a normoglycemic state,

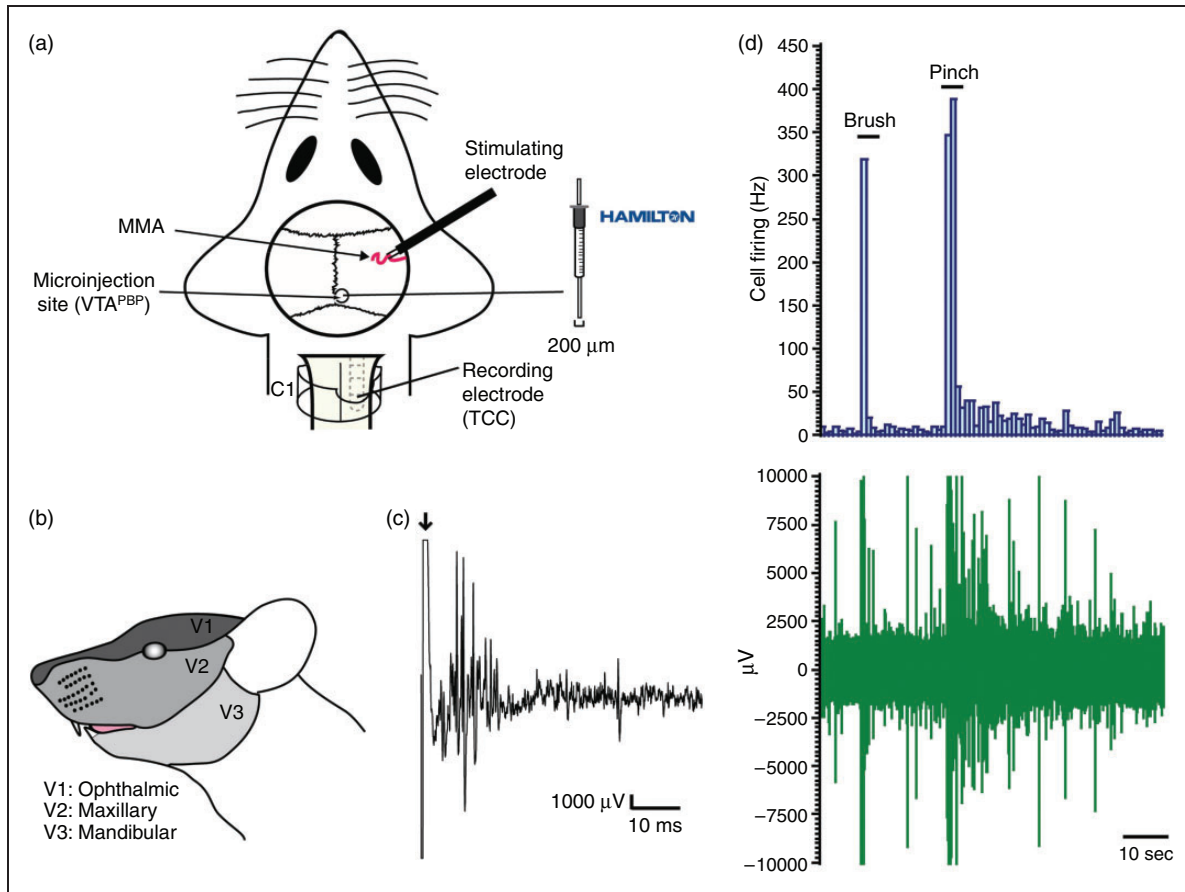


**Figure 1.** Overview of the experimental setup and neuronal characteristics.

(a) Experimental setup with dural electrical stimulation, recording of neurons in the TCC and VTA<sup>PBP</sup> microinjections. (b) All neurons studied were wide dynamic range (WDR); responsive to both noxious and innocuous stimulation, with cutaneous receptive field in the first (V1; ophthalmic) division of the trigeminal nerve. (c) An original tracing from a typical unit (second-order neuron) responding to electrical stimulation of the dura mater adjacent to the MMA (latencies in the A $\delta$ -fiber range). Black arrow represents stimulus artefact and (d) Original example of the electrophysiological neuronal response to innocuous brush and noxious pinch of the cutaneous V1 receptive field. Bottom panel is original electrophysiological output, top panel is responses that cross the window discriminator. C1, spinal cord cervical 1; MMA, middle meningeal artery; TCC, trigeminocervical complex; VTA<sup>PBP</sup>, parabrachial pigmented nucleus of the ventral tegmental area.

animals were assessed after induction anesthesia and before surgical preparation. Blood glucose levels were then quantified at two specific time-points: before inserting the recording electrode and the microinjection syringe into the brain, and at 60 min post-microinjection, as described (35).

### Postsurgical examination of tissue

Animals were euthanized and an electrothermolytic lesion was made in the TCC. Brains and spinal cord were removed and sliced (60- $\mu$ m and 40- $\mu$ m-thick coronal sections) on a freezing cryostat. The exact microinjection sites were verified using a light microscope (Axioplan Microscope; Carl Zeiss) and the rat brain atlas (22).

### Experimental design and statistical analysis

Trains of 20 stimuli were delivered at 5 min intervals to assess the baseline response to dural electrical stimulation. Data collected for A $\delta$ -fibers represent the normalized data for the number of cells firing over a 10 ms period in the region 4–20 ms post-stimulation over the 20 sweeps. Responses were analyzed using post-stimulus histograms with a sweep length of 100 ms and a bin width of 1 ms that separated A $\delta$ -fiber-activated firing. When stable baseline values of the dural-evoked responses were achieved and cutaneous and deep receptive field inputs from the ophthalmic division of the trigeminal nerve were obtained, responses were tested for up to 60 min following microinjections. Ongoing spontaneous trigeminal neuronal

activity (spikes/second, Hz) was recorded continuously, and data related to 120–150 sec preceding the dural stimulation using peri-stimulus histograms was analyzed, as described (50). This activity was analyzed as cumulative rate histograms in which neuronal activity gated through the amplitude discriminator was collected into successive bins.

Two types of mechanical stimuli were delivered to the ipsilateral ophthalmic dermatome of the trigeminal nerve: 1) innocuous brushing and 2) noxious pinching, as described previously (50). Responses were recorded immediately before, and 15, 30 and 60 min after microinjection. Only one baseline for the mechanical stimuli was taken to avoid sensitization prior to drug administration. Spontaneous discharges were documented for 5 sec after application of the stimulus and the mean firing rate (Hz) response to each mechanical stimulus was analyzed. Data is expressed as mean  $\pm$  SEM and the mean firing rate upon application of each stimulus prior to drug microinjection was taken to be 100%. Using previous experience (35), a minimum of seven animals were used in electrophysiological studies to measure time points up to 60 min.

Statistical analysis was performed in raw data using IBM SPSS (v23.0). To detect whether there was a significant effect over time (pre-injection and eight individual time point values at 5, 10, 15, 20, 25, 30, 45 and 60 min post-injection) we used one-way ANOVA for repeated measures (RM-ANOVA) with Bonferroni *post-hoc* correction for multiple comparisons, using a 95% confidence interval. If Mauchly's test of sphericity was violated, appropriate corrections to the degrees of freedom were made according to Greenhouse–Geisser (51). Student's paired *t*-test (two-tailed) was used for *post-hoc* analysis of individual time points comparing to pre-injection values. To compare the treatment group (bicuculline) with the vehicle treatment group we used two-way repeated measures ANOVA with a Greenhouse-Geisser correction and Tukey's test for *post-hoc* analysis. Statistical significance was set at  $P < 0.05$  level. The experimenter was aware of (not blinded to) each step of the experimental process.

## Results

### Serotonin and PACAP receptors are present in the VTA<sup>PBP</sup>

Given that antibodies can be nonspecific, we assume a putative expression herein. Putative 5-HT<sub>1B</sub> and 5-HT<sub>1D</sub> receptors (green labelling) were present within the VTA<sup>PBP</sup>, with 5-HT<sub>1B</sub> receptors more visible associated with fibers, whereas 5-HT<sub>1D</sub> receptors with cell bodies (Figure 2A, 2D). These receptors were also present in the paraventricular nucleus of the

hypothalamus (PVN), and the substantia nigra, compact part, dorsal tier (SNCD) (Figure 2B, 2E). Putative receptors for PACAP, namely PAC<sub>1</sub>, VPAC<sub>1</sub> and VPAC<sub>2</sub> receptors (red labelling), were distributed throughout all levels of the VTA<sup>PBP</sup> region (Figure 3A, 3D, 3F). These receptors were also present in other brain structures: the red nucleus, parvicellular part (RPC), the arcuate nucleus of the hypothalamus (ARC) and the PAG (Figure 3B, 3E, 3G). All receptors were colocalized with DAPI (nuclear marker; blue), indicating its presence in cell bodies. No specific staining was observed when the primary antibody was omitted (Figure 2C and Figure 3C).

### In vivo electrophysiology experiments

*Physiology parameters, electrophysiological data, and postsurgical histology.* A total of 49 animals had microinjections inside the VTA<sup>PBP</sup>, a mean body weight of  $301 \pm 2$  g and blood glucose levels within physiological levels at the beginning of the experiment ( $6.33 \pm 0.06$  mmol/L). Data from animals in which histological analysis showed microinjection placements outside the VTA<sup>PBP</sup> ( $n = 21$ ) were excluded from the main analysis.

Extracellular recordings in the TCC were made from a total of 54 neurons. In animals that received a second microinjection ( $n = 4$ , vehicle control;  $n = 1$ , bicuculline) there was a washout period of 90–120 min. Neurons responding to dural electrical stimulation responded with an average latency of  $10.6 \pm 0.2$  ms (range 4–20 ms, Figure 1C shows an example of evoked neuronal firing) and were classified as A $\delta$ -fibers. Very few C-fiber latency (beyond 20 ms) responses were observed, and therefore we were only able to quantify A $\delta$ -fiber responses. Most neurons were in lamina V of the dorsal horn of the cervicomedullary junction, with 13 neurons in lamina II–IV, at an average depth of  $588 \pm 23$   $\mu$ m and the electrode placement was confirmed in all animals (Figure S1A and S1B). The mean ongoing spontaneous firing rate pre-injection (baseline) was  $28 \pm 2.3$  Hz (range 1.8–64.8 Hz), with most neurons responding between 5 and 25 Hz; this is within the same range as previously demonstrated (44). The location of microinjections inside the VTA<sup>PBP</sup> (black dots) and adjacent to the VTA<sup>PBP</sup> (black stars) are indicated in representative atlas plate rat brain sections (22) (Figure S1C) and histological example in Figure S1D.

*Glutamatergic stimulation of the VTA<sup>PBP</sup> reduces nociceptive and spontaneous TCC neuronal firing.* Glutamate significantly inhibited dural-evoked responses ( $F_{2,3,16,3} = 4.615$ ;  $P = 0.022$ ;  $n = 8$ ) (Figure 4A, S2A) and spontaneous neuronal firing ( $F_{2,1,15,3} = 8.372$ ;  $P = 0.003$ ;  $n = 8$ ) (Figure 4B). Moreover, bicuculline significantly

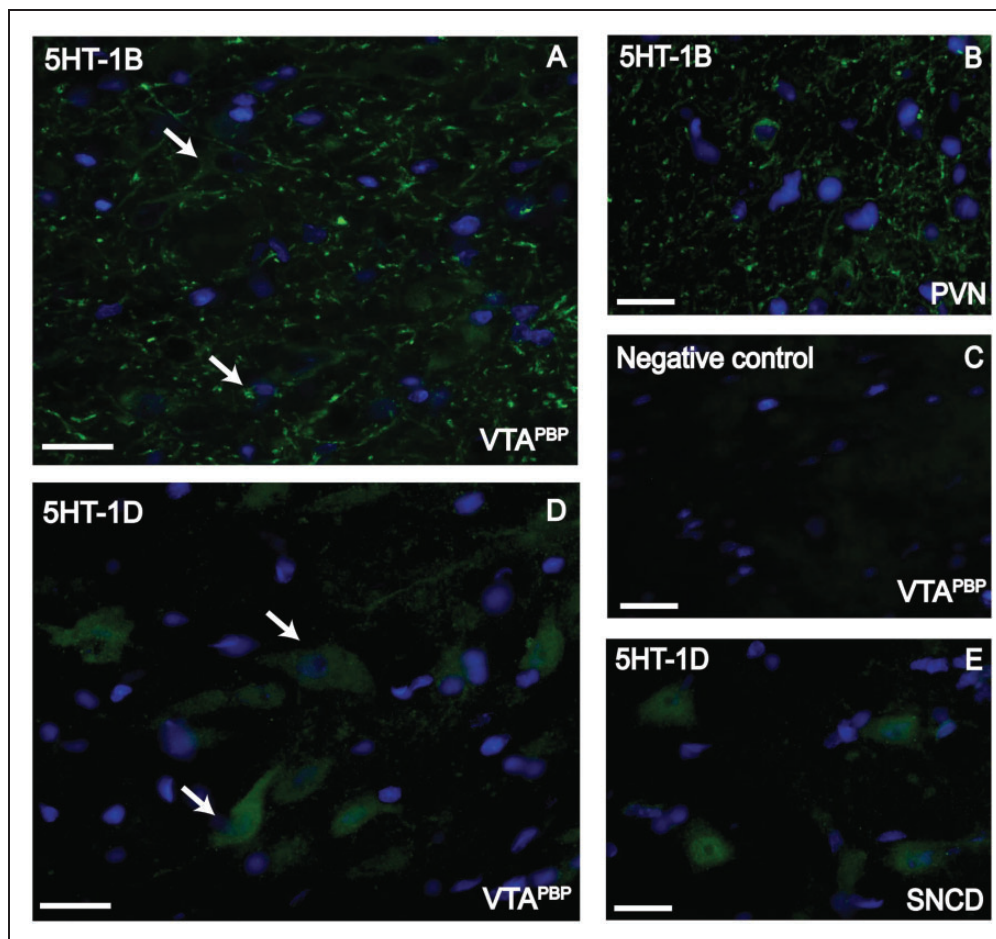


**Figure 2.** Immunofluorescence staining for 5HT<sub>1B</sub> and 5HT<sub>1D</sub> receptors in the VTA<sup>PBP</sup>. (a) 5HT<sub>1B</sub> receptors in the VTA<sup>PBP</sup> (green); (b) 5HT<sub>1B</sub> receptors in the paraventricular nucleus of the hypothalamus (PVN), as positive control (green); (c) Negative control in the VTA<sup>PBP</sup>, obtained by omitting the primary antibodies; (d) 5HT<sub>1D</sub> receptors in the VTA<sup>PBP</sup> (green) and (e) 5HT<sub>1D</sub> receptors in the substantia nigra, compact part, dorsal tier (SNCD) (green), as a positive control; Receptors are colocalized with DAPI (blue, nuclear marker). Arrows indicate examples in each image. Scale bars, 20  $\mu$ m.

reduced dural-evoked neuronal firing within the TCC ( $F_{2.4,24.6} = 3.791$ ;  $P = 0.029$ ;  $n = 11$ ) (Figure 4A, S2A), however had no significant effect on the ongoing spontaneous activity when compared to pre-injection ( $F_{2.8,28.2} = 1.229$ ;  $P = 0.316$ ;  $n = 11$ ) (Figure 4B). Microinjection of vehicle control in the VTA<sup>PBP</sup> had no significant effect on A $\delta$ -fiber responses ( $F_{4.2,46} = 2.030$ ;  $P = 0.102$ ;  $n = 12$ ) (Figure 4A, S2A) and on ongoing spontaneous activity ( $F_{3.5,39} = 2.596$ ;  $P = 0.056$ ;  $n = 12$ ) of trigeminal second-order neurons (Figure 4B). Given that the bicuculline treatment group showed greater variance in ongoing spontaneous responses, we aimed to confirm whether the larger variance may have affected the meaning of the results (one-way RM-ANOVA did not show significance throughout the 60 min experiment). We further compared spontaneous firing responses between vehicle control and bicuculline treatment and a two-way RM-ANOVA revealed that the main effect of

treatment group on the average spontaneous firing responses across time was not statistically significant ( $F_{1,21} = 2.958$ ,  $p = 0.1$ ).

A summary of ongoing spontaneous firing rate after 5 and 10 min for each treatment group is presented in Table S1.

*Naratriptan and PACAP38 modulation of VTA<sup>PBP</sup> inhibits nociceptive and spontaneous TCC neuronal firing.* Microinjection of naratriptan into the VTA<sup>PBP</sup> significantly reduced dural-evoked neuronal firing within the TCC ( $F_{2.9,20.7} = 12.163$ ;  $P = 0.000$ ;  $n = 8$ ) (Figure 4C, S2B) and had a significant inhibitory effect on the ongoing spontaneous activity ( $F_{2.0,14.2} = 5.616$ ;  $P = 0.015$ ;  $n = 8$ ) (Figure 4D). Similarly, PACAP38 significantly reduced dural-evoked neuronal firing within the TCC ( $F_{1.7,10.6} = 9.392$ ;  $P = 0.005$ ;  $n = 7$ ) (Figure 4C, S2B), and ongoing spontaneous activity ( $F_{1.3,8.1} = 7.872$ ;  $P = 0.017$ ;  $n = 7$ ) (Figure 4D). Moreover, quinpirole

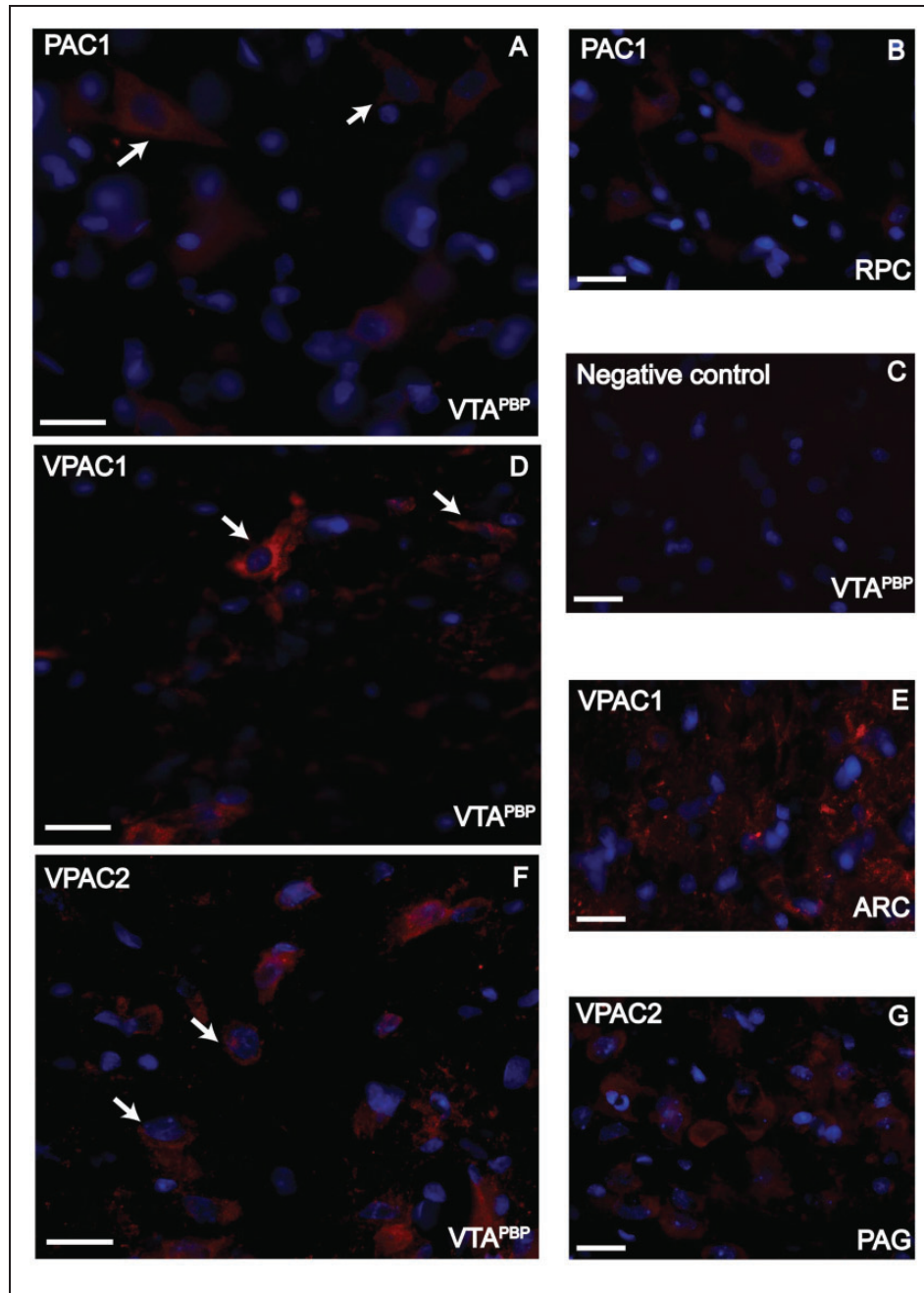


**Figure 3.** Immunofluorescence staining for PAC<sub>1</sub>, VPAC<sub>1</sub> and VPAC<sub>2</sub> receptors in the VTA<sup>PBP</sup>. (a) PAC<sub>1</sub> receptors in the VTA<sup>PBP</sup> (red); (b) PAC<sub>1</sub> receptors in the red nucleus, parvicellular part (RPC), as a positive control (red); (c) Negative control in the VTA<sup>PBP</sup>, obtained by omitting the primary antibodies. (d) VPAC<sub>1</sub> receptors in the VTA<sup>PBP</sup> (red); (e) VPAC<sub>1</sub> receptors in the arcuate nucleus of the hypothalamus (ARC), as a positive control (red); (f) VPAC<sub>2</sub> receptors in the VTA<sup>PBP</sup> (red) and (g) VPAC<sub>2</sub> receptors in the periaqueductal gray (PAG), as a positive control (red); Receptors are colocalized with DAPI (blue, nuclear marker). Arrows indicate examples in each image. Scale bars, 20  $\mu$ m.

significantly reduced dural-evoked neuronal firing within the TCC ( $F_{3,6,25,8} = 7.005$ ;  $P = 0.001$ ;  $n = 8$ ) (Figure 4C, S2B), and ongoing spontaneous activity ( $F_{3,1,21,9} = 3.491$ ;  $P = 0.031$ ;  $n = 8$ ) (Figure 4D). A summary of ongoing spontaneous firing rate after 5 and 10 min for each treatment group is presented in Table S1.

*Naratriptan and PACAP38 modulation of VTA<sup>PBP</sup> reduced innocuous and noxious facial TCC responses.* Measurements of neuronal responses to cutaneous mechanical stimulation of the ophthalmic dermatome were made from 45 neurons. Data from the recordings of nine neurons were excluded from this analysis due to incomplete

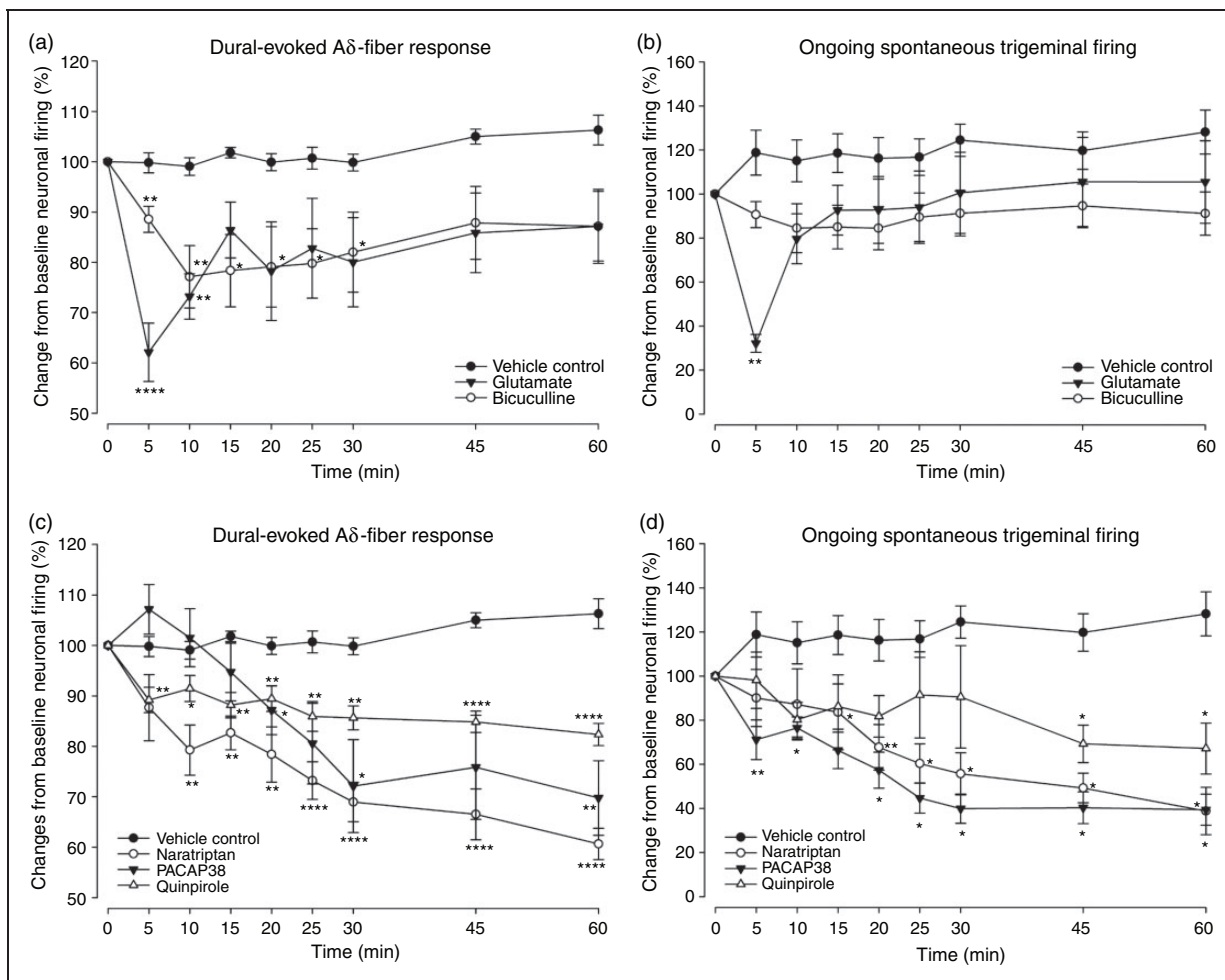


**Figure 4.** Effects of pharmacological manipulation of VTA<sup>PBP</sup> on dural-evoked and spontaneous neuronal firing in the trigemino-cervical complex (TCC).

(a) Time course changes in the average response of dural-evoked A $\delta$ -fiber trigeminal neuronal firing following microinjection of glutamate ( $n=8$ ) and bicuculline ( $n=11$ ), which significantly decreased neuronal responses by a maximum of 38% and 23%, respectively. (b) Time course of ongoing spontaneous trigeminal neuronal firing in response to glutamate ( $n=8$ ), which significantly decreased neuronal responses by a maximum of 68% at 5 min and then recovered, and bicuculline ( $n=11$ ), which had no significant effect compared to pre-injection levels. (c) Time course of the average response of intracranial dural-evoked A $\delta$ -fiber trigeminal neuronal firing following microinjection of naratriptan ( $n=8$ ), PACAP38 ( $n=7$ ) and quinpirole ( $n=8$ ), which significantly decreased neuronal responses by a maximum of 39%, 30% and 18%, respectively and (d) Time course of spontaneous trigeminal neuronal firing in response to naratriptan ( $n=8$ ), PACAP38 ( $n=7$ ) and quinpirole ( $n=8$ ), which significantly decreased neuronal responses by a maximum of 61%, 60% and 33%, respectively. In all panels vehicle control ( $n=12$ ) had no significant effects of neuronal responses. Data have been normalized to represent the percentage change from baseline, and are expressed as means  $\pm$  SEM. \* $P < 0.05$ ; \*\* $P < 0.01$ ; \*\*\* $P < 0.001$ ; \*\*\*\* $P < 0.0001$ .

data collection for one or more time points of the experimental design ( $n=1$ , vehicle control;  $n=7$ , bicuculline;  $n=1$ , glutamate). Vehicle control had no significant effect on responses to either innocuous brush ( $F_{3,30}=0.964$ ;  $P=0.422$ ;  $n=11$ ) (Figure 5A) or noxious pinch ( $F_{3,30}=0.607$ ;  $P=0.615$ ;  $n=11$ ) (Figure 5B) of cutaneous facial receptive fields. For both glutamate and bicuculline, there were no effects in response to innocuous brush (Glu:  $F_{3,18}=1.037$ ;  $P=0.400$ ;  $n=7$ ; bicuculline:  $F_{3,9}=1.895$ ;  $P=0.201$ ;  $n=4$ ). Both

significantly reduced responses to noxious pinch (Glu:  $F_{3,18}=5.132$ ;  $P=0.010$ ;  $n=7$ ; bicuculline:  $F_{3,9}=12.169$ ;  $P=0.002$ ;  $n=4$ ) (Figure 5B). Naratriptan significantly inhibited neuronal responses to innocuous brush ( $F_{3,21}=7.516$ ;  $P=0.001$ ;  $n=8$ ) (Figure 5A) and noxious pinch ( $F_{1,5,10,8}=12.602$ ;  $P=0.002$ ;  $n=8$ ) (Figure 5C). Similarly, PACAP38 significantly inhibited responses to innocuous brush ( $F_{3,18}=5.248$ ;  $P=0.009$ ;  $n=7$ ) (Figure 5A) and noxious pinch ( $F_{1,1,6,9}=5.622$ ;  $P=0.047$ ;  $n=7$ ) (Figure 5C).



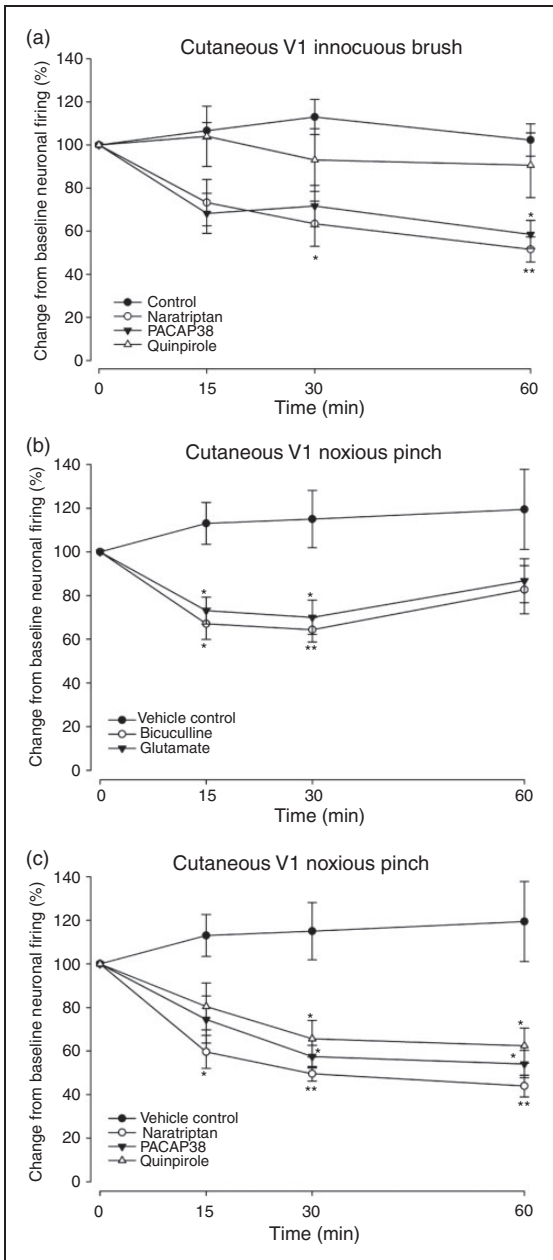


**Figure 5.** Effect of VTA<sup>PBP</sup> pharmacological modulation on neuronal firing in the trigemino-cervical complex (TCC), in response to mechanical stimulation of the ophthalmic dermatome (V1).

Time course changes in the average response of TCC neurons to somatosensory-evoked stimulation of the cutaneous facial receptive field. (a) response to innocuous brush stimulation following microinjection of naratriptan ( $n = 8$ ), PACAP38 ( $n = 7$ ) and quinpirole ( $n = 8$ ) into the VTA<sup>PBP</sup>; (b) response to noxious pinch stimulation following microinjection of glutamate ( $n = 7$ ) and bicuculline ( $n = 4$ ) into the VTA<sup>PBP</sup>; and (c) response to noxious pinch stimulation following microinjection of naratriptan ( $n = 8$ ), PACAP38 ( $n = 7$ ) and quinpirole ( $n = 8$ ) into the VTA<sup>PBP</sup>. In all panels vehicle control ( $n = 11$ ) had no significant effects of neuronal responses. Data have been normalized to represent the percentage change from baseline, and are expressed as means  $\pm$  SEM. \* $p < 0.05$ ; \*\* $p < 0.01$ .

Furthermore, quinpirole did not affect innocuous responses ( $F_{3,21} = 0.587$ ;  $P = 0.630$ ;  $n = 8$ ) (Figure 5A), but significantly inhibited responses to noxious pinch ( $F_{1,4,10,4} = 7.322$ ;  $P = 0.014$ ;  $n = 8$ ) (Figure 5C).

### Trigeminovascular processing through VTA<sup>PBP</sup> modulation results in reduced blood glucose levels

In all experiments, blood glucose was within physiological levels before microinjection of drugs ( $5.47 \pm 0.09$  mmol/L). Data from 48 experiments were analyzed, and in animals that received two microinjections, blood glucose measures were only taken after the first microinjection. Modulation with glutamate significantly decreased blood glucose levels by 11% ( $t_7 = 2.981$ ;  $P = 0.020$ ;  $n = 8$ ), an effect mimicked by bicuculline ( $t_9 = 3.641$ ;  $P = 0.005$ ;  $n = 10$ ). Furthermore, naratriptan VTA<sup>PBP</sup> modulation significantly decreased blood glucose levels by 12% ( $t_7 = 2.443$ ;  $P = 0.045$ ;  $n = 8$ ) and PACAP38 induced a significant blood glucose level reduction of 17% ( $t_6 = 2.731$ ;  $P = 0.034$ ;  $n = 7$ ). There were no significant effects on blood glucose levels following microinjection of quinpirole ( $t_7 = 0.082$ ;  $P = 0.937$ ;  $n = 8$ ) or vehicle control ( $t_6 = 1.485$ ;  $P = 0.188$ ;  $n = 7$ ). Blood glucose levels before and 60 min following VTA<sup>PBP</sup> microinjection are presented in Table S2.

## Discussion

We show that pharmacological modulation of the VTA<sup>PBP</sup> is sufficient to alter the transmission of trigeminovascular nociceptive and innocuous inputs. Whether VTA<sup>PBP</sup> activity is necessary for physiological trigeminovascular sensory processing is unknown, yet our findings and others showing VTA activation in human imaging of migraine (3) and VTA involvement in aversive behavior in an inflammatory model of headache (8) suggest that the VTA may be relevant to understand associated sensory and homeostatic symptoms in susceptible migraine patients. Anatomical studies (9,52) do not report direct VTA projections to the TCC, therefore the effects of VTA<sup>PBP</sup> manipulation on TCC neuronal responses can be explained by indirect action on relay stations, namely the NAc, PAG, PVN or lateral hypothalamus (LH) (45,53).

We showed that excitatory and inhibitory inputs to the VTA<sup>PBP</sup> inhibit trigeminovascular neuronal responses. Within the VTA, there are two general populations of GABA neurons: interneurons, which provide local inhibition of DA neurons, and projection neurons, which provide long-range inhibition of multiple brain areas including the NAc, the prefrontal cortex, the lateral habenula, lateral hypothalamus, preoptic area, and amygdala, as well as to structures in the

thalamus, midbrain, pons, and medulla (14,54,55). Importantly, these VTA GABA neurons are known to express the GABA<sub>A</sub> receptor (55–57). Given the current literature (6,11,57–59), possible explanations could account for the effects of the GABA<sub>A</sub> receptor antagonist (bicuculline): 1) Effects directly on VTA<sup>PBP</sup> Daergic neurons expressing GABA<sub>A</sub> receptors, preventing GABAergic inhibition, and thereby increasing Daergic firing (thus inducing a similar response to glutamate VTA<sup>PBP</sup> microinjection); 2) Effects on VTA GABA interneurons, facilitating its firing and thereby increasing inhibitory input to VTA<sup>PBP</sup> DA neurons, resulting in inhibition of the mesolimbic DA system; 3) Effects on GABAergic VTA<sup>PBP</sup> long-range projection neurons, facilitating its firing, leading to increased inhibition of target structures (e.g. NAc, prefrontal cortex, central amygdala, dorsal raphe nucleus, among other regions). Although many of these projections have been identified anatomically, there has been little functional characterization of cellular properties of these neurons or synaptic properties of their terminals and projection neurons may have local collaterals, allowing coordination of VTA activity with activity in distal target regions (60). Overall, given that DA neurons represent 65% of and GABA neurons 30% of VTA neurons (11), one can hypothesize that the effects observed herein are likely to be mediated through VTA<sup>PBP</sup> Daergic neurons expressing GABA<sub>A</sub> receptors.

Of note, it has been difficult to disentangle the function of DA neurons and GABA neurons, and between local VTA GABA neurons and GABAergic projection neurons (extensively reviewed elsewhere (59,60)). In addition, VTA neurons release various combinations of DA, GABA, and glutamate, all of which form local and long-range connections (9,15,25,52,61). Therefore, to gain a full understanding of the likely neuronal circuitry underlying the responses herein, it is imperative to gain genetic access to these cells (e.g. opto- or chemogenetics) in future studies of migraine pathophysiology.

### **Naratriptan and PACAP38 in the VTAPBP exert similar effects in TCC neuronal firing**

Naratriptan in the VTA<sup>PBP</sup> inhibits TCC neuronal firing through 5-HT<sub>1B/1D</sub> receptors, putatively present throughout this structure. Consistent with our findings, naratriptan has similar effects when microinjected into the vlPAG (47), PVN (45), A11 (34) and infused peripherally (44). Given that serotonin is implicated in reward processing (62) and naratriptan-induced 5-HT<sub>1B/1D</sub> receptor activation is able to block nociceptive pathways, our findings support the rewarding effect of pain relief.

Unexpectedly, PACAP38 in the VTA<sup>PBP</sup> reduced all types of TCC activities. These results are challenging given that PACAP38 administered intravenously induces delayed sensitization of central trigeminovascular neurons (50), which translates to delayed migraine-like headaches in 50% of migraine patients without aura (33). In animals, PACAP38 in the PVN does not modify A $\delta$ -fiber responses but increases TCC spontaneous activity (45). Nonetheless, PACAP's role in pain transmission is complex, with studies showing both anti- and pro-nociceptive actions (63,64). In our study, the precise mechanisms through which intra-VTA<sup>PBP</sup> PACAP38 inhibits TCC responses are unknown, although the differences on nociceptive behavior might be receptor dependent.

The immunohistochemistry in our study showed the putative expression of three PACAP receptors specifically within the VTA<sup>PBP</sup>. Previously, *in situ* hybridization revealed a wide distribution of PACAP-R mRNA with intense-to-moderate labeling in the VTA (30), yet an immunoreactive study showed no expression above background density level for PAC<sub>1</sub>, <40% of maximal level for VPAC<sub>1</sub>, and <80% of maximal level for VPAC<sub>2</sub> (32).

Regarding peptide brain expression, soma that contain PACAP are relatively restricted to selected regions of the limbic system and brainstem, yet fibers containing PACAP and levels of PACAP protein are found in the VTA (65). To date, it is known that major PACAP inputs to the VTA originate from the hypothalamic ventromedial nucleus (VMN) and these neurons inhibit the excitability of VTA dopaminergic neurons *via* activation of PAC<sub>1</sub> receptors and K<sub>ATP</sub> channels (66). Conversely, vasoactive intestinal peptide (VIP), which shows 68% sequence homology with PACAP and acts on the same receptors (although PAC<sub>1</sub> shows much greater affinity for PACAP than for VIP) (67), is highly expressed in the VTA (68–70) and is co-expressed with TH in the VTA<sup>PBP</sup> (68).

While we confirm PAC<sub>1</sub>, VPAC<sub>1</sub> and VPAC<sub>2</sub> receptors are “putatively” present specifically within the VTA<sup>PBP</sup>, it has been suggested PACAP pro-nociceptive actions are likely mediated *via* PAC<sub>1</sub> receptor (71) and anti-nociceptive, anti-hyperalgesic and anti-allodynic effects mediated by VPAC<sub>1</sub> and VPAC<sub>2</sub> receptors (72). Therefore, additional studies (e.g. knock-out receptor) are needed to clarify this mechanism.

Moreover, recent studies provide evidence that PACAP plays an important role in reward processing, such as modulation of the rewarding and reinforcing actions of addictive drugs (65). PACAP in specific limbic brain regions can promote reward seeking and intake and itself is stimulated by their intake (65). Although the expression and wide distribution of

PAC<sub>1</sub> and/or VPAC receptors contribute to the broad and diverse actions of PACAP, the stress- and addiction-related responses of PACAP appear to be mediated predominantly by the PACAP-selective PAC<sub>1</sub> receptor (73). Of note, there is a close relationship between reward/aversion and pain relief/pain mediated by the mesolimbic reward circuitry that involves the mesolimbic DA emanating from the VTA and projecting to the NAc (74,75). It has been also postulated that removal of an aversive state is rewarding (76). Indeed, relief of pain produces negative reinforcement through activation of the mesolimbic reward-valuation circuitry. In specific, activation of VTA dopaminergic neurons and release of DA as well as activation of dopaminergic receptors in the NAc mediates the reinforcing effect of pain relief (74,77,78). Given the role of PACAP on motivated behaviors in response to addictive drugs and that addiction behavior is associated with reward anticipation (e.g. craving), it is possible that PACAP, predominantly *via* the PAC<sub>1</sub> receptor, may likely contribute to a mechanism of reward processing and craving involving inhibition of nociceptive responses as a way of termination of the aversive stimulus. However, we cannot exclude the fact that PACAP binds with high affinity to PAC<sub>1</sub> and VPAC<sub>1</sub> and VPAC<sub>2</sub>, and given this overlap, it will be important to dissect which receptor is mediating a given PACAP effect.

Regarding DA signaling, quinpirole administration in the VTA<sup>PBP</sup> inhibited TCC neuronal firing; an effect supported by systemic studies (34). Dopamine D<sub>2</sub>-like receptors are important in pain modulation (79) and exert auto-inhibitory somatodendritic effects (80). Thus, if quinpirole is likely to induce auto-inhibitory actions on DA neurons and, herein, inhibited TCC noxious inputs, it is possible VTA<sup>PBP</sup> non-DA neurons (e.g. GABAergic neurons) could have influenced TCC nociceptive processing in our experiments.

Overall, clinical-relevant drugs in the VTA<sup>PBP</sup> modulate both spontaneous and dural-evoked activities of TCC neurons suggesting its effects are not nociceptive-specific. Given that modulation of VTA<sup>PBP</sup> neuronal activity is sufficient to elicit changes in trigeminovascular sensory processing, it is possible that, in susceptible persons, VTA<sup>PBP</sup> neurons could alter trigeminovascular processing by integrating nociceptive, as well as other processing mechanisms (e.g. hedonic or homeostatic). In addition, the modulatory influences of VTA<sup>PBP</sup> on both spontaneous and dural-evoked TCC activities could be mediated by different top-down mechanisms promoted by the varied neuronal populations within the VTA<sup>PBP</sup>.

The VTA is known to process mechanical inputs through DAergic mechanisms (81). We show that VTA<sup>PBP</sup> modulation by naratriptan and PACAP38

alters responses to facial mechanical stimulation, which may be relevant for underlying allodynia and hyperalgesia mechanisms in susceptible patients. Interestingly, a previous study has demonstrated a relationship between DA and 5-HT within the TCC *via* DA-projecting A11 neurons, where lesioning the A11 facilitates noxious facial-evoked inputs, and both systemic 5-HT<sub>1B/1D</sub> and D<sub>2</sub> receptor agonists reverse this (34). Thus, it is possible that a similar synergistic relationship occurs as well in the TCC *via* VTA<sup>PBP</sup>.

### *Modulation of the VTA<sup>PBP</sup> impacts post-trigeminovascular processing glycemia*

Trigeminovascular sensory processing through VTA<sup>PBP</sup> modulation is accompanied by reduced blood glucose levels. We have previously shown that dural-evoked TCC neuronal firing is modulated by systemic glucoregulatory peptides and TCC pERK1/2 cell expression is decreased by insulin and increased by glucagon (35). Moreover, disturbances in glucose and insulin metabolism have been reported in migraine patients, namely impaired insulin sensitivity (extensively reviewed elsewhere (28)).

These electrophysiological studies were carried out in anesthetized animals, yet we confirmed a normoglycemic state within physiological levels, ruling out possible anesthetic-induced variations.

We hypothesize that the reduced blood glucose levels may occur due to specific metabolic effects triggered by VTA<sup>PBP</sup> modulation and its outcomes on projection targets. Possible metabolic effects include increased insulin secretion, increased expression of insulin sensitive glucose transporters (GLUTs), increased insulin-mediated suppression of endogenous glucose production, and improved insulin sensitivity with stimulation of glucose utilization in peripheral tissues. To our knowledge, none of these have been studied as an effect of VTA neuronal activity. Although the VTA neuronal firing is influenced by glucoregulatory peptides, including insulin (82,83) and glucagon-like peptide-1 (GLP-1) (84,85), there is no evidence reporting VTA neuronal activity direct effects on systemic glucose levels. More recently, however, it has been shown that NAc neuronal activity (a known VTA projection target) seems to regulate systemic glucose metabolism by increasing insulin sensitivity (86). Given the current available literature, we may speculate the NAc could potentially be a relay station explaining the reduced glucose levels observed in our study.

Moreover, naratriptan and PACAP are known to influence glycemia. Serotonin interacts with glucose metabolism (87) and induces a dose-dependent serum insulin increase and serum glucose decrease in mice (88,89); whereas in obese diabetic animals and diabetic

humans serotonergic drugs improve glucose tolerance and insulin sensitivity (90–92). PACAP is synthesized and released by pancreatic  $\beta$ -cells and exerts several metabolic actions, such as stimulation of insulin production and release, and increase of insulin-induced glucose uptake in adipocytes, thereby improving glucose tolerance (93–95). It is possible that improved insulin sensitivity may accompany naratriptan and PACAP-38 antinociceptive effects in our study. Whether there is a nociceptive-specific glucoregulatory mechanism in migraine remains to be established.

Physiologically, blood glucose changes may lead to appetite changes. In susceptible migraine patients, the interplay between VTA<sup>PBP</sup> activity and the sensory processing by the trigeminovascular system may be relevant to understand associated sensory and homeostatic symptoms. Our findings may provide plausible groundwork biology to unravel appetite changes in susceptible migraine patients.

### Further research and implications

Given that VTA is a heterogeneous nucleus containing dopaminergic (DA) neurons (9), as well as GABAergic

and GLU neurons (10–12), additional experiments could dissect the co-localization of 5-HT<sub>1</sub> and PACAP receptors with either TH, Glu or GABAergic neurons, providing more information on the likely neuronal circuitry mediating PACAP and naratriptan effects on VTA<sup>PBP</sup> neurons.

Furthermore, a technical constraint of the study is that the methodology used herein does not unravel the likely neuronal circuitry mediating PACAP and naratriptan effects on VTA<sup>PBP</sup> neurons. For instance, brain slice recordings could provide additional information, such as identification of the VTA<sup>PBP</sup> neuronal type being modulated by these drugs. In addition, a direct input from the VTA to the TCC is currently unknown. Regardless, it has been shown in an animal model of orofacial pain, that stimulation of the NAc inhibited nociceptive trigeminal nucleus caudalis neurons mediated by NAc dopamine D2 receptors and transmitted through the rostral ventromedial medulla (96). Given the known VTA<sup>PBP</sup>-NAc projections, future experiments could incorporate pathway-specific manipulation of this brain circuitry in a migraine animal model by using opto- or chemogenetics.

### Article highlights

- Modulation of VTA<sup>PBP</sup> neuronal activity is sufficient to alter the transmission of trigeminovascular nociceptive and innocuous inputs.
- Serotonin and PACAP receptors are putatively expressed within the VTA<sup>PBP</sup> region.
- Naratriptan, PACAP38, quinpirole intra-VTA<sup>PBP</sup> inhibit trigeminovascular responses.
- Trigeminal sensory processing through VTA<sup>PBP</sup> modulation is accompanied by reduced blood glucose levels.

### Acknowledgments

The authors would like to thank Jessika Bridi and Michele Lasalandra for technical advice on immunohistochemistry experiments. Alomone Labs, Israel, kindly provided antibody samples.

### CRediT Author Statement

**Margarida Martins-Oliveira:** Conceptualization, Methodology, Formal analysis, Investigation, Writing – Original Draft, Writing – Review & Editing, Visualization, Funding acquisition.

**Simon Akerman:** Conceptualization, Methodology, Supervision, Writing – Review & Editing, Project administration.

**Philip R Holland:** Conceptualization, Methodology, Supervision, Writing – Review & Editing, Project administration, Funding acquisition.

**Isaura Tavares:** Conceptualization, Methodology, Supervision, Writing – Review & Editing, Project administration, Funding acquisition.

**Peter J Goadsby:** Conceptualization, Methodology, Supervision, Writing – Review & Editing, Project administration, Funding acquisition.

### Conflict of interest statement



The authors declared the following potential conflicts of interest with respect to the research, authorship, and/or publication of this article: MMO (margaridamartinsoliveira.phd@gmail.com; margarida.martinsoliveira@nms.unl.pt) declares no competing financial interests. SA (sakerman@umaryland.edu) reports, unrelated to this work, personal fees from Amgen, Novartis, GSK, and Patent Legal work in headache. PRH (philip.holland@kcl.ac.uk) reports, unrelated to this work, grants from Amgen and Eli Lilly and company as well as honoraria and travel expenses in relation to educational duties from Allergan, Novartis, Teva and Almirall. IT (isatav@med.up.pt) declares no competing financial interests. PJG reports, over the last 36 months, grants and personal fees from Amgen and Eli-Lilly and Company, grant from Celgene, and personal fees from

Alder Biopharmaceuticals, Allergan, Aeon Bopharma., Biohaven Pharmaceuticals Inc., Clexio, Electrocore LLC, eNeura, Epalex, Impel Neuropharma, MundiPharma, Novartis, Sanofi, Santara Therapeutics, Satsuma, Teva Pharmaceuticals, Trigemina Inc., WL Gore, and personal fees from MedicoLegal work, Massachusetts Medical Society, Up-to-Date, Oxford University Press, and Wolters Kluwer; and a patent magnetic stimulation for headache assigned to eNeura without fee.

### Funding

The authors disclosed receipt of the following financial support for the research, authorship, and/or publication of this article: Margarida Martins-Oliveira is grateful to the Portuguese Fundação para a Ciência e Tecnologia (FCT) for its support with an individual PhD grant (SFRH/BD/77127/2011). The conduct of the research was financially supported by the EUROHEADPAIN European Union FP7 (PJG & PRH: 602633), the Wellcome Trust (PJG: 104033) and the Medical Research Council (PRH: MR/P006264/1).

### ORCID iDs

Simon Akerman  <https://orcid.org/0000-0002-6577-6825>  
Peter J Goadsby  <https://orcid.org/0000-0003-3260-5904>

### References

- Denuelle M, Fabre N, Payoux P, et al. Hypothalamic activation in spontaneous migraine attacks. *Headache* 2007; 47: 1418–1426.
- Schulte LH and May A. The migraine generator revisited: continuous scanning of the migraine cycle over 30 days and three spontaneous attacks. *Brain* 2016; 139: 1987–1993.
- Maniyar FH, Sprenger T, Monteith T, et al. Brain activations in the premonitory phase of nitroglycerin-triggered migraine attacks. *Brain* 2014; 137: 232–241.
- Mercer Lindsay N, Chen C, Gilam G, et al. Brain circuits for pain and its treatment. *Sci Transl Med* 2021; 13: eabj7360.
- Ferrario CR, Labouèbe G, Liu S, et al. homeostasis meets motivation in the battle to control food intake. *J Neurosci* 2016; 36: 11469–11481.
- Morales M and Margolis EB. Ventral tegmental area: cellular heterogeneity, connectivity and behaviour. *Nat Rev Neurosci* 2017; 18: 73–85.
- Hsu TM, McCutcheon JE and Roitman MF. Parallels and overlap: the integration of homeostatic signals by mesolimbic dopamine neurons. *Front Psychiatry* 2018; 9: 410.
- Wang MW, Margolis EB, Charbit AR, et al. A mid-brain circuit that mediates headache aversiveness in rats. *Cell Rep* 2019; 28: 2739–2747.e2734.
- Swanson LW. The projections of the ventral tegmental area and adjacent regions: a combined fluorescent retrograde tracer and immunofluorescence study in the rat. *Brain Res Bull* 1982; 9: 321–353.
- Dobi A, Margolis EB, Wang HL, et al. Glutamatergic and nonglutamatergic neurons of the ventral tegmental area establish local synaptic contacts with dopaminergic and nondopaminergic neurons. *J Neurosci* 2010; 30: 218–229.
- Margolis EB, Toy B, Himmels P, et al. Identification of rat ventral tegmental area GABAergic neurons. *PLoS One* 2012; 7: e42365.
- Yamaguchi T, Sheen W and Morales M. Glutamatergic neurons are present in the rat ventral tegmental area. *Eur J Neurosci* 2007; 25: 106–118.
- Nair-Roberts RG, Chatelain-Badie SD, Benson E, et al. Stereological estimates of dopaminergic, GABAergic and glutamatergic neurons in the ventral tegmental area, substantia nigra and retrorubral field in the rat. *Neuroscience* 2008; 152: 1024–1031.
- Taylor SR, Badurek S, Dileone RJ, et al. GABAergic and glutamatergic efferents of the mouse ventral tegmental area. *J Comp Neurol* 2014; 522: 3308–3334.
- Morales M and Root DH. Glutamate neurons within the midbrain dopamine regions. *Neuroscience* 2014; 282C: 60–68.
- Fields HL, Hjelmstad GO, Margolis EB, et al. Ventral tegmental area neurons in learned appetitive behavior and positive reinforcement. *Annu Rev Neurosci* 2007; 30: 289–316.
- Gorelova N, Mulholland PJ, Chandler LJ, et al. The glutamatergic component of the mesocortical pathway emanating from different subregions of the ventral mid-brain. *Cereb Cortex* 2012; 22: 327–336.
- Yamaguchi T, Wang HL, Li X, et al. Mesocorticolimbic glutamatergic pathway. *J Neurosci* 2011; 31: 8476–8490.
- Hnasko TS, Hjelmstad GO, Fields HL, et al. Ventral tegmental area glutamate neurons: electrophysiological properties and projections. *J Neurosci* 2012; 32: 15076–15085.
- Sanchez-Catalan MJ, Kauffling J, Georges F, et al. The antero-posterior heterogeneity of the ventral tegmental area. *Neuroscience* 2014; 282C: 198–216.
- Oades RD and Halliday GM. Ventral tegmental (A10) system: neurobiology. 1. Anatomy and connectivity. *Brain Res* 1987; 434: 117–165.
- Paxinos G and Watson C. *The Rat Brain in Stereotaxic Coordinates*. 5th ed. San Diego, California: Elsevier Academic Press, 2005.
- Mazei-Robison MS and Nestler EJ. Opiate-induced molecular and cellular plasticity of ventral tegmental area and locus coeruleus catecholamine neurons. *Cold Spring Harb Perspect Med* 2012; 2: a012070.
- Lammel S, Hetzel A, Häckel O, et al. Unique properties of mesoprefrontal neurons within a dual mesocorticolimbic dopamine system. *Neuron* 2008; 57: 760–773.
- Lammel S, Ion DI, Roeper J, et al. Projection-specific modulation of dopamine neuron synapses by aversive and rewarding stimuli. *Neuron* 2011; 70: 855–862.
- Yang H, de Jong JW, Tak Y, et al. Nucleus accumbens subnuclei regulate motivated behavior via direct inhibition and disinhibition of VTA dopamine subpopulations. *Neuron* 2018; 97: 434–449.e434.
- Giffin NJ, Ruggiero L, Lipton RB, et al. Premonitory symptoms in migraine: an electronic diary study. *Neurology* 2003; 60: 935–940.

28. Martins-Oliveira M, Tavares I and Goadsby PJ. Was it something I ate? Understanding the bidirectional interaction of migraine and appetite neural circuits. *Brain Res* 2021; 147629. DOI: 10.1016/j.brainres.2021.147629.
29. Goadsby PJ, Holland PR, Martins-Oliveira M, et al. Pathophysiology of migraine: A disorder of sensory processing. *Physiol Rev* 2017; 97: 553–622.
30. Hashimoto H, Nogi H, Mori K, et al. Distribution of the mRNA for a pituitary adenylate cyclase-activating polypeptide receptor in the rat brain: an in situ hybridization study. *J Comp Neurol* 1996; 371: 567–577.
31. Pazos A and Palacios JM. Quantitative autoradiographic mapping of serotonin receptors in the rat brain. I. Serotonin-1 receptors. *Brain Res* 1985; 346: 205–230.
32. Joo KM, Chung YH, Kim MK, et al. Distribution of vasoactive intestinal peptide and pituitary adenylate cyclase-activating polypeptide receptors (VPAC1, VPAC2, and PAC1 receptor) in the rat brain. *J Comp Neurol* 2004; 476: 388–413.
33. Schytz HW, Birk S, Wienecke T, et al. PACAP38 induces migraine-like attacks in patients with migraine without aura. *Brain* 2009; 132: 16–25.
34. Charbit AR, Akerman S and Goadsby PJ. Trigemino-cervical complex responses after lesioning dopaminergic A11 nucleus are modified by dopamine and serotonin mechanisms. *Pain* 2011; 152: 2365–2376.
35. Martins-Oliveira M, Akerman S, Holland PR, et al. Neuroendocrine signaling modulates specific neural networks relevant to migraine. *Neurobiol Dis* 2017; 101: 16–26.
36. Martins-Oliveira M, Akerman S, Holland P, et al. Midbrain reward pathway and premonitory food craving in migraineurs: studies in a animal model. *Cephalalgia* 2016; 36: 1–185.
37. Martins-Oliveira M, Akerman S, Holland PR, et al. Pleasure and pain: exploring neurobiological mechanisms of food craving before migraine pain. *Cephalalgia* 2017; 37: 1–378.
38. Kilkenny C, Browne W, Cuthill IC, et al. Animal research: reporting in vivo experiments: the ARRIVE guidelines. *Br J Pharmacol* 2010; 160: 1577–1579.
39. Zimmermann M. Ethical guidelines for investigations of experimental pain in conscious animals. *Pain* 1983; 16: 109–110.
40. Pommer S, Akamine Y, Schiffmann SN, et al. The effect of serotonin receptor 5-HT1B on lateral inhibition between spiny projection neurons in the mouse striatum. *J Neurosci* 2021; 41: 7831–7847.
41. Varodayan FP, Minnig MA, Steinman MQ, et al. PACAP regulation of central amygdala GABAergic synapses is altered by restraint stress. *Neuropharmacol* 2020; 168: 107752.
42. Minnig MA, Park T, Echeveste Sanchez M, et al. Viral-mediated knockdown of nucleus accumbens shell pacl receptor promotes excessive alcohol drinking in alcohol-preferring rats. *Front Behav Neurosci* 2021; 15: 787362.
43. Ivic I, Balasko M, Fulop BD, et al. VPAC1 receptors play a dominant role in PACAP-induced vasorelaxation in female mice. *PLoS One* 2019; 14: e0211433.
44. Martins-Oliveira M, Akerman S, Tavares I, et al. Neuropeptide Y inhibits the trigeminovascular pathway through NPY Y1 receptor: implications for migraine. *Pain* 2016; 157: 1666–1673.
45. Robert C, Bourgeois L, Arreto CD, et al. Paraventricular hypothalamic regulation of trigeminovascular mechanisms involved in headaches. *J Neurosci* 2013; 33: 8827–8840.
46. Knight YE, Bartsch T and Goadsby PJ. Trigeminal antinociception induced by bicuculline in the periaqueductal gray (PAG) is not affected by PAG P/Q-type calcium channel blockade in rat. *Neurosci Lett* 2003; 336: 113–116.
47. Bartsch T, Knight YE and Goadsby PJ. Activation of 5-HT(1B/1D) receptor in the periaqueductal gray inhibits nociception. *Ann Neurol* 2004; 56: 371–381.
48. Zhang DG, Amin FM, Guo S, et al. Plasma glucose levels increase during spontaneous attacks of migraine with and without aura. *Headache* 2020; 60: 655–664.
49. Rainero I, Limone P, Ferrero M, et al. Insulin sensitivity is impaired in patients with migraine. *Cephalalgia* 2005; 25: 593–597.
50. Akerman S and Goadsby PJ. Neuronal PAC1 receptors mediate delayed activation and sensitization of trigemino-cervical neurons: Relevance to migraine. *Sci Transl Med* 2015; 7: 308ra157.
51. Field A. *Discovering Statistics Using SPSS*. 4 ed. London: SAGE, 2013.
52. Aransay A, Rodríguez-López C, García-Amado M, et al. Long-range projection neurons of the mouse ventral tegmental area: a single-cell axon tracing analysis. *Front Neuroanat* 2015; 9: 59.
53. Becerra L, Navratilova E, Porreca F, et al. Analogous responses in the nucleus accumbens and cingulate cortex to pain onset (aversion) and offset (relief) in rats and humans. *J Neurophysiol* 2013; 110: 1221–1226.
54. van Zessen R, Phillips JL, Budygin EA, et al. Activation of VTA GABA neurons disrupts reward consumption. *Neuron* 2012; 73: 1184–1194.
55. Tan KR, Yvon C, Turiault M, et al. GABA neurons of the VTA drive conditioned place aversion. *Neuron* 2012; 73: 1173–1183.
56. Tan KR, Brown M, Labouèbe G, et al. Neural bases for addictive properties of benzodiazepines. *Nature* 2010; 463: 769–774.
57. Ciccarelli A, Calza A, Panzanelli P, et al. Organization of GABAergic synaptic circuits in the rat ventral tegmental area. *PLoS One* 2012; 7: e46250.
58. Ikemoto S, Kohl RR and McBride WJ. GABA(A) receptor blockade in the anterior ventral tegmental area increases extracellular levels of dopamine in the nucleus accumbens of rats. *J Neurochem* 1997; 69: 137–143.
59. Creed MC, Ntamati NR and Tan KR. VTA GABA neurons modulate specific learning behaviors through the control of dopamine and cholinergic systems. *Front Behav Neurosci* 2014; 8: 8. 20140122.
60. Bouarab C, Thompson B and Polter AM. VTA GABA neurons at the interface of stress and reward. *Front Neural Circuits* 2019; 13: 78.

61. Lammel S, Lim BK, Ran C, et al. Input-specific control of reward and aversion in the ventral tegmental area. *Nature* 2012; 491: 212–217.
62. Kranz GS, Kasper S and Lanzenberger R. Reward and the serotonergic system. *Neuroscience* 2010; 166: 1023–1035.
63. Sándor K, Kormos V, Botz B, et al. Impaired nocifensive behaviours and mechanical hyperalgesia, but enhanced thermal allodynia in pituitary adenylate cyclase-activating polypeptide deficient mice. *Neuropeptides* 2010; 44: 363–371.
64. Shimizu T, Katahira M, Sugawara H, et al. Diverse effects of intrathecal pituitary adenylate cyclase-activating polypeptide on nociceptive transmission in mice spinal cord. *Regul Pept* 2004; 123: 117–122.
65. Gargiulo AT, Curtis GR and Barson JR. Pleiotropic pituitary adenylate cyclase-activating polypeptide (PACAP): Novel insights into the role of PACAP in eating and drug intake. *Brain Res* 2020; 1729: 146626.
66. Le N, Hernandez J, Gastelum C, et al. Pituitary adenylate cyclase activating polypeptide inhibits A10 dopamine neurons and suppresses the binge-like consumption of palatable food. *Neuroscience* 2021; 478: 49–64.
67. Harmar AJ, Fahrenkrug J, Gozes I, et al. Pharmacology and functions of receptors for vasoactive intestinal peptide and pituitary adenylate cyclase-activating polypeptide: IUPHAR review 1. *Br J Pharmacol* 2012; 166: 4–17.
68. Tiklová K, Björklund Å, Lahti L, et al. Single-cell RNA sequencing reveals midbrain dopamine neuron diversity emerging during mouse brain development. *Nat Commun* 2019; 10: 581.
69. Poulin JF, Gaertner Z, Moreno-Ramos OA, et al. Classification of midbrain dopamine neurons using single-cell gene expression profiling approaches. *Trends Neurosci* 2020; 43: 155–169.
70. Chung CY, Seo H, Sonntag KC, et al. Cell type-specific gene expression of midbrain dopaminergic neurons reveals molecules involved in their vulnerability and protection. *Hum Mol Genet* 2005; 14: 1709–1725.
71. Yokai M, Kurihara T and Miyata A. Spinal astrocytic activation contributes to both induction and maintenance of pituitary adenylate cyclase-activating polypeptide type 1 receptor-induced long-lasting mechanical allodynia in mice. *Mol Pain* 2016; 12. DOI: 10.1177/1744806916646383.
72. Sándor K, Bölskei K, McDougall JJ, et al. Divergent peripheral effects of pituitary adenylate cyclase-activating polypeptide-38 on nociception in rats and mice. *Pain* 2009; 141: 143–150.
73. Miles OW, May V and Hammack SE. Pituitary Adenylate Cyclase-Activating Peptide (PACAP) signaling and the dark side of addiction. *J Mol Neurosci* 2019; 68: 453–464.
74. Navratilova E and Porreca F. Reward and motivation in pain and pain relief. *Nat Neurosci* 2014; 17: 1304–1312.
75. Lammel S, Lim BK and Malenka RC. Reward and aversion in a heterogeneous midbrain dopamine system. *Neuropharmacology* 2014; 76 Pt B: 351–359.
76. Tanimoto H, Heisenberg M and Gerber B. Experimental psychology: event timing turns punishment to reward. *Nature* 2004; 430: 983.
77. De Felice M, Eyde N, Dodick D, et al. Capturing the aversive state of cephalic pain preclinically. *Ann Neurol* 2013; 74: 257–265.
78. Navratilova E, Xie JY, Okun A, et al. Pain relief produces negative reinforcement through activation of mesolimbic reward-valuation circuitry. *Proc Natl Acad Sci U S A* 2012; 109: 20709–20713.
79. Moradi M, Yazdani M and Haghparast A. Role of dopamine D2-like receptors within the ventral tegmental area and nucleus accumbens in antinociception induced by lateral hypothalamus stimulation. *Behav Brain Res* 2015; 292: 508–514.
80. Beckstead MJ, Grandy DK, Wickman K, et al. Vesicular dopamine release elicits an inhibitory postsynaptic current in midbrain dopamine neurons. *Neuron* 2004; 42: 939–946.
81. Sogabe S, Yagasaki Y, Onozawa K, et al. Mesocortical dopamine system modulates mechanical nociceptive responses recorded in the rat prefrontal cortex. *BMC Neurosci* 2013; 14: 65.
82. Liu S and Borgland SL. Regulation of the mesolimbic dopamine circuit by feeding peptides. *Neuroscience* 2015; 289: 19–42.
83. Mebel DM, Wong JC, Dong YJ, et al. Insulin in the ventral tegmental area reduces hedonic feeding and suppresses dopamine concentration via increased reuptake. *Eur J Neurosci* 2012; 36: 2336–2346.
84. Konanur VR, Hsu TM, Kanoski SE, et al. Phasic dopamine responses to a food-predictive cue are suppressed by the glucagon-like peptide-1 receptor agonist Exendin-4. *Physiol Behav* 2020; 215: 112771.
85. Dickson SL, Shirazi RH, Hansson C, et al. The glucagon-like peptide 1 (GLP-1) analogue, exendin-4, decreases the rewarding value of food: a new role for mesolimbic GLP-1 receptors. *J Neurosci* 2012; 32: 4812–4820.
86. Ter Horst KW, Lammers NM, Trinko R, et al. Striatal dopamine regulates systemic glucose metabolism in humans and mice. *Sci Transl Med* 2018; 10. DOI: 10.1126/scitranslmed.aar3752.
87. McGlashon JM, Gorecki MC, Kozlowski AE, et al. Central serotonergic neurons activate and recruit thermogenic brown and beige fat and regulate glucose and lipid homeostasis. *Cell Metab* 2015; 21: 692–705.
88. Yamada J, Sugimoto Y, Kimura I, et al. Serotonin-induced hypoglycemia and increased serum insulin levels in mice. *Life Sci* 1989; 45: 1931–1936.
89. Sugimoto Y, Kimura I, Yamada J, et al. Effects of serotonin on blood glucose and insulin levels of glucose- and streptozotocin-treated mice. *Jpn J Pharmacol* 1990; 54: 93–96.
90. Arora R, Dryden S, McKibbin PE, et al. Acute dexfenfluramine administration normalizes glucose tolerance in rats with insulin-deficient diabetes. *Eur J Clin Invest* 1994; 24: 182–187.
91. Gomez R, Huber J, Tombini G, et al. Acute effect of different antidepressants on glycemia in diabetic and non-diabetic rats. *Braz J Med Biol Res* 2001; 34: 57–64.

92. Maheux P, Ducros F, Bourque J, et al. Fluoxetine improves insulin sensitivity in obese patients with non-insulin-dependent diabetes mellitus independently of weight loss. *Int J Obes Relat Metab Disord* 1997; 21: 97–102.
93. Yada T, Sakurada M, Ihida K, et al. Pituitary adenylate cyclase activating polypeptide is an extraordinarily potent intra-pancreatic regulator of insulin secretion from islet beta-cells. *J Biol Chem* 1994; 269: 1290–1293.
94. Nakata M, Shioda S, Oka Y, et al. Insulinotropin PACAP potentiates insulin-stimulated glucose uptake in 3T3 L1 cells. *Peptides* 1999; 20: 943–948.
95. Nakata M and Yada T. PACAP in the glucose and energy homeostasis: physiological role and therapeutic potential. *Curr Pharm Des* 2007; 13: 1105–1112.
96. Barceló AC, Filippini B and Pazo JH. The striatum and pain modulation. *Cell Mol Neurobiol* 2012; 32: 1–12.